A Pilot-Correlated PMD Monitoring Scheme for Direct Detection Optical OFDM System

Tianwai Bo, Shuang Gao, Kam-Hon Tse, and Chun-Kit Chan, *Senior Member, IEEE*

***Abstract*—A polarization mode dispersion monitoring scheme is proposed and demonstrated for direct-detection optical orthogonal frequency division multiplexing (DDO-OFDM) systems. A pair of data-assisted pilot subcarriers is inserted at two spectral edges of the OFDM signal spectrum. Simple data correlation technique is used to estimate the powers of the pilot subcarriers and thus retrieves the DGD value at the monitoring unit, without the need of demodulation of the pilot subcarriers. Experiments show a DGD monitoring range of 0 to 45 ps in a typical radio-frequency tone-assisted DDO-OFDM system. The robustness of the proposed scheme to optical signal-to-noise ratio and accumulated chromatic dispersion is further experimentally investigated. Besides, simulations and experiments are performed to demonstrate the feasibility of using photodiodes with narrow bandwidth. By inserting one more data-assisted pilot subcarrier, the proposed scheme becomes insensitive to the input angle of the state of polarization. The proposed scheme provides an effective monitoring solution for the optical OFDM signals across intermediate nodes in flexible optical network.**

***Index Terms*—Digital signal processing, optical fiber communication, optical performance monitoring.**

I. Introduction

RECENTLY, flexible optical network has been widely recognized as a promising approach to support future high-speed heterogeneous data traffic [1]. Optical orthogonal frequency division multiplexing (OFDM) is one of the feasible candidates to enable such flexible network, for its flexible bandwidth and high spectral efficiency [2]. To date, there are two mainstreams of optical OFDM systems, in terms of the signal detection technique, namely coherent optical OFDM (CO-OFDM) [3] and direct detection optical OFDM (DDO-OFDM) [4]. In medium/short distance transmission, such as metro/access networks, DDO-OFDM is more preferred because of its low requirement for transmitter's laser linewidth [5]. It employs a cost-effective photodiode, instead of expensive coherent receivers, to achieve high speed transmission, though at certain expense of sensitivity. As reported in [6], super-channel DDO-OFDM with 432-Gb/s, 3040-km single mode fiber transmission has been experimentally demonstrated, highlighting the good potential of DDO-OFDM even in long haul transmission. However, it suffers from a critical drawback of power fading induced by the chromatic dispersion (CD) and polarization mode dispersion (PMD) of fiber link, due to the square law of photodiode. Generally, the frequency-dependent power fading reduces the signal power of the optical subcarriers at higher frequencies, and this degrades the performance of DDO-OFDM system [7]. Single side band (SSB) modulation can remove the power fading induced by chromatic dispersion [8] but does no help to PMD-induced power fading. Moreover, simulations have shown that PMD induces significant performance degradation in optical OFDM system with commonly used single polarization photodiode [9]. Therefore, monitoring of the PMD is indispensable in DDO-OFDM based flexible optical networks. In order to assure the quality of the optical OFDM signals over an optical network, low-cost and effective in-line optical performance monitoring (OPM) techniques are highly desirable to be incorporated at the intermediate network nodes, such that the network control plane can be kept updated of the optical signal quality, for the subsequent compensation.

Recently, there have been some interesting schemes reported to monitor the differential group delay (DGD), which characterizes the first order PMD effect, for CO-OFDM signals. In [10], a coherent receiver was used to estimate the channel response of the CO-OFDM signal, and the DGD value was derived from the inverse of the fading period in the channel response. In [11], the Stokes vectors for symbols on each optical subcarrier of a CO-OFDM signal were calculated without any aided data. As the PMD-induced state of polarization (SOP) rotation generates an arc on the Poincaré sphere, the DGD value could be derived from the angle of arc divided by the frequency difference of the optical subcarriers. In [12], we have recently proposed a code-correlation based PMD monitoring method for an up-converted DDO-OFDM system, in which a pair of code-assisted pilot subcarriers was employed to monitor the PMD value.

In this paper, we have further performed extensive experimental characterization of the proposed scheme in a 10-Gb/s DDO-OFDM system with a signal bandwidth of 5.5 GHz. The robustness of the proposed monitoring techniques to optical signal-to-noise ratio (OSNR) and chromatic dispersion is investigated. Furthermore, we have demonstrated that the bandwidth of photodiode (PD) used in this scheme can be as low as 1 GHz, which further reduces the cost. The proposed scheme shows strong tolerance to the amplified spontaneous emission (ASE) noise and chromatic dispersion in the fiber transmission link. Besides, by inserting one more data-assisted pilot subcarrier, the proposed scheme becomes insensitive to the input angle of the signal's state of polarization (SOP). The proposed scheme offers a robust and effective solution to realize in-line PMD monitoring for future high-speed flexible optical network.

Manuscript received February 2, 2015; revised March 17, 2015; accepted March 30, 2015. Date of publication April 5, 2015; date of current version May 22, 2015. This work was supported in part by a grant from Hong Kong Research Grants Council (General Research Fund: CUHK410512).

The authors are with the Department of Information Engineering, Chinese University of Hong Kong, Shatin, Hong Kong (e-mail: bt012@ie.cuhk.edu.hk; gs012@ie.cuhk.edu.hk; tkh008@ie.cuhk.edu.hk; ckchan@ie.cuhk.edu.hk).

Color versions of one or more of the figures in this paper are available online at http://ieeexplore.ieee.org.

Digital Object Identifier 10.1109/JLT.2015.2420532

The rest of the paper is organized as follows. Section II illustrates the principle of proposed pilot-correlated PMD monitoring scheme in DDO-OFDM. Section III presents the experimental demonstration. Robustness to other impairments such as ASE noise and CD are investigated in this section. Section IV presents the theoretical and experimental analyses the PMD monitoring scheme using low-bandwidth PDs, a modified scheme which is insensitive to the input angle of the signal's SOP and a brief discussion on the issue of polarization dependent loss (PDL). Finally, section V summarizes the paper.

II. PMD Monitoring Principle

A. PMD Induced Power Fading

As the SOP of an optical signal rotates based on the DGD and frequency, each frequency component of the subcarrier of optical OFDM signal will have a relative difference in SOP with the optical carrier after fiber transmission. It is not a critical issue in a CO-OFDM system, in which a coherent receiver is used. However, when only a photodiode is used to detect the DDO-OFDM signal, the optical carrier and the optical signal will beat, according to the square law of the photodiode detection. The misalignment of the SOPs among the optical carrier and the optical subcarriers creates destructive interference among themselves during the signal beating, which leads to power fading over the entire power spectrum of the detected signal, characterized by (1) [13],

$$H(\omega_k, \gamma, \Delta\tau) = \gamma + (1-\gamma)e^{-j\omega_k \Delta\tau} \tag{1}$$

where γ is the amplitude splitting ratio, $\omega_k (= 2\pi f_k)$ is the angular frequency difference between the optical carrier and the k^{th} optical subcarrier residing at frequency f_k.$\Delta\tau$ is the DGD value of the fiber link. In (1), if γ equals 0.5, in which the input optical signal is equally split into two orthogonal principal states of polarization (PSPs), and using frequency difference instead of angular frequency difference, the DGD gives the highest impact on the optical signal and (1) becomes,

$$|H(f_k, \Delta\tau)| = |\cos(\pi f_k \Delta\tau)| \tag{2}$$

Owing to the relatively flat power spectrum of the input optical OFDM signal, such cosine-like PMD-induced power fading would be imposed over the whole signal's spectrum. Hence, the DGD value of fiber can be derived from the spectrum, which is of the cosine function, as in (2). To derive the DGD value $\Delta\tau$, at least the amplitudes of the two frequencies, within the same period of the cosine function, should be known, as illustrates in Fig. 1, We have

$$A_1 = a_1 \cos(\pi f_1 \Delta\tau) \tag{3}$$

$$A_2 = a_2 \cos(\pi f_2 \Delta\tau) \tag{4}$$

where f_1 and f_2 are two different frequency components of the OFDM signal, A_1 and A_2 are the corresponding amplitudes. a_1 and a_2 are the corresponding ideal magnitudes of the OFDM signal transfer function without DGD, and are identical in general. By combining (3) and (4), we have,

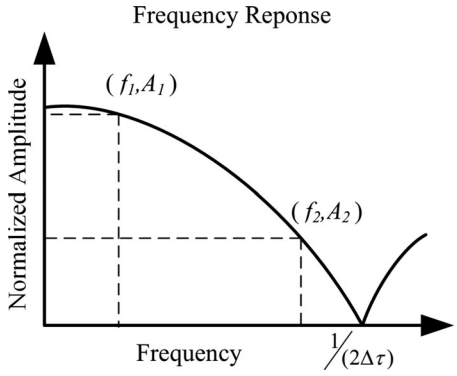

Fig. 1. Channel response of the PMD induced power fading characterized by (2).

$$\cos(\pi f_1 \Delta\tau) = q \cdot \cos(\pi f_2 \Delta\tau) \tag{5}$$

where q is the ratio of A_1 to A_2. If the values of f_1, f_2, A_1 and A_2 are known, the unknown parameter $\Delta\tau$ can be easily derived, via (5). A straightforward solution of estimating the amplitudes of the frequency components is to use an RF spectrum analyzer, which is expensive. Here, we propose a simple method based on data correlation technique to determine the amplitudes, A_1 and A_2, in order to derive the DGD value, $\Delta\tau$.

B. Using Inserted Pilots to Monitor 1st Order PMD

In a DDO-OFDM system, data can be freely modulated onto a certain optical subcarrier. Two distinct pilot sequences are loaded to the first and the last subcarrier of the OFDM signal, respectively, via inverse fast Fourier transform (IFFT). If the IFFT size is N, that is, there are N samples in one OFDM symbol, the OFDM symbol in time domain can be expressed, as follows:

$$s(n) = \frac{1}{N}\sum_{k=1}^{N} S(k) e^{j2\pi \frac{k}{N} \cdot n} \tag{6}$$

where $S(k)$ is the information carried on the k^{th} subcarrier of the OFDM symbol. Consider the i^{th} subcarrier in the m^{th} OFDM symbol is loaded with a designated pilot data $C(m)$, that is, $S_m(i) = C(m)$. $C(m)$ can be regarded as a pilot subcarrier. At the receiver, a pilot signal $c(n)$, which is generated by padding all the subcarriers to be zero except the i^{th} subcarrier set to be $C(m)$. The time domain expression of the pre-defined sequence is:

$$c_m(n) = \frac{1}{N} C(m) e^{j2\pi \frac{i}{N} \cdot n} \tag{7}$$

For M OFDM symbols, by applying signal correlation procedure between the OFDM signal, $s(n)$, and the regenerated pilot sequence, $c(n)$, the maximum correlation value is calculated, as

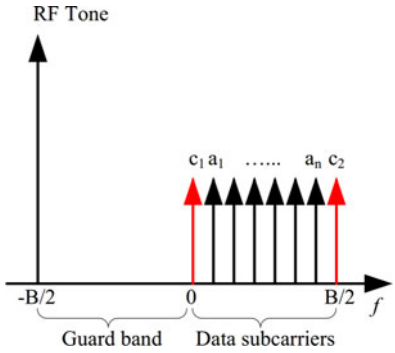

Fig. 2. Pilot and data arrangement in frequency domain. a_1 to a_n (black) are normal data subcarriers, while c_1 and c_2 (red) are pilot subcarriers. B is the bandwidth of OFDM signal.

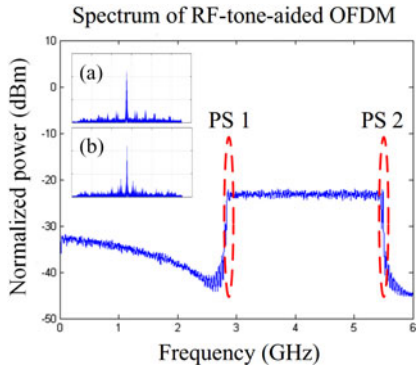

Fig. 3. Simulation result of frequency spectrum of direct detected RF-tone-assisted OFDM signal. The red circles mark the position of two inserted pilot subcarriers (PS). Insets are the correlation peaks for (a) pilot 1 and (b) pilot 2 when correlation is performed when DGD set to be 0 ps in simulation.

follows:

$$\begin{aligned} R_{\max} &= \sum_{m=1}^{M} \frac{1}{N^2} \sum_{n=1}^{N} s_m^*(n)\, c_m(n) \\ &= \sum_{m=1}^{M} \frac{1}{N^2} \sum_{n=1}^{N} \sum_{k=1}^{N} S_m(k)^* e^{-j2\pi \frac{k}{N} \cdot n} C(m) e^{j2\pi \frac{i}{N} \cdot n} \\ &= \sum_{m=1}^{M} \frac{1}{N^2} \left(\sum_{n=1}^{N} S_m(i)^* e^{-j2\pi \frac{k}{N} \cdot n} C(m) e^{j2\pi \frac{i}{N} \cdot n} \right. \\ &\quad \left. + \sum_{n=1}^{N} \sum_{\substack{k=1 \\ k \neq i}}^{N} S_m(k)^* e^{-j2\pi \frac{k}{N} \cdot n} C(m) e^{j2\pi \frac{i}{N} \cdot n} \right) \end{aligned} \tag{8}$$

The second term in (8) will become zero, as arbitrary two subcarriers are orthogonal. With $S_m(i) = C(m)$, the maximum correlation value of *M* OFDM symbols is

$$R_{\max} = \frac{1}{N} \sum_{m=1}^{M} |C(m)|^2 \tag{9}$$

which corresponds to the average power of the pilot data sequence $C(m)$, loaded at the i^{th} subcarrier. This shows the feasibility of using the peak magnitude of the pilot correlation result to estimate the power of a certain frequency component. As the amplitude response for all subcarriers is relatively constant with time, except for the random fluctuations caused by the ASE noise [8], averaging over several OFDM symbols makes the power estimation result more accurate.

With the effectiveness of using signal correlation to estimate the average power of the pilot data sequences loaded onto a subcarrier in an OFDM signal, we propose to load two distinct pilot symbol sequences with the same average power as the other data-modulated subcarriers, into the OFDM signal, one at each end of the signal spectrum, as depicted in Fig. 2, so as to estimate the DGD value accumulated in the received DDO-OFDM signal. The data are modulated in quadrature amplitude modulated (QAM) format. The generated OFDM signal is then modulated by a conventional RF-tone aided optical OFDM [14] modulator to form the DDO-OFDM signal for transmission.

At the receiver, in order to estimate the average power of the designated pilot data sequence loaded at the first optical subcarrier of the received DDO-OFDM signal, a time-domain pilot signal is generated by loading the same designated pilot data sequence to the respective subcarrier, with other subcarriers padded to zeroes, via IFFT. The pilot data sequence can be stored in the monitoring module in advance, so as to alleviate the computation requirement. Signal correlation operation is then performed between this pilot signal and the received DDO-OFDM signal so as to estimate the average received power of the first designated pilot data sequence. The same procedure is repeated by generating another pilot signal, which corresponds to the designated pilot data sequence loaded to the last optical subcarrier of the DDO-OFDM signal, and correlating it with the received DDO-OFDM signal in order to estimate the average received power of the second designated pilot data sequence. Fig. 3 shows the respective simulated correlation spectra after the signal correlation procedures have been performed for the two designated pilot sequences, showing prominent correlation peaks and their peak magnitudes are the same under zero DGD value. Hence, with the known frequencies of those two pilot subcarriers, together with the estimated values their respective amplitudes, via the proposed correlation procedures, the DGD value accumulated on the DDO-OFDM signal can be derived, via (5).

Here we use a searching algorithm to find the zero value of $g(\Delta\tau)$ in (10) when the frequency values and the power ratio are obtained.

$$g(\Delta\tau) = \cos(\pi f_1 \Delta\tau) - q \cdot \cos(\pi f_2 \Delta\tau) \tag{10}$$

A step is set first which defines the resolution of DGD calculation. $g(\Delta\tau)$ is calculated for a linear increment of $\Delta\tau$, until zero value occurs. The corresponding $\Delta\tau$ is the resolved DGD value. The computation complexity is determined by the resolution and monitoring range. For example, for a monitoring range of 45 ps and a resolution of 0.1 ps, the maximum number of searching attempts is 450, in the worst case. In real-time implementation, if the frequencies of the pilot subcarriers are fixed, a simple lookup table method could be used to reduce

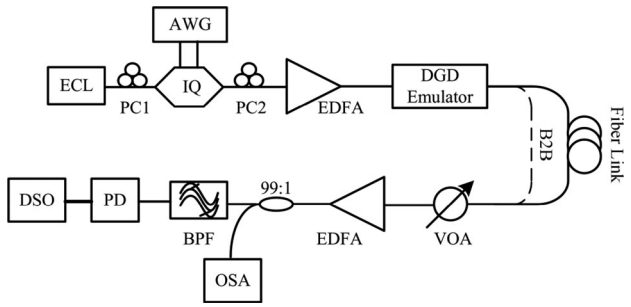

Fig. 4. Experimental setup. ECL: external cavity diode laser; AWG: arbitrary waveform generator; VOA: variable optical attenuator; OSA: optical spectrum analyzer; DSO: digital storage oscilloscope; PD: photodiode; PC: polarization controller; BPF: band-pass filter; IQ: in-phase/quadrature modulator; B2B: back-to-back.

the computation complexity in real-time implementation. The respective DGD values for each power ratio under certain resolution were pre-computed and stored in the look-up table. In the monitoring scheme, after the correlation procedure is performed and the power ratio is obtained, the respective DGD value could be directly retrieved, via the lookup table.

It is noted that deriving DGD value, via (10), has ambiguity, as it is a periodic function and has a series of solutions. A simple and effective solution is to limit the searching range of the possible DGD values. It is due to the fact that for signal with a certain bandwidth Δf, the maximum monitored DGD is determined by $1/(2\cdot\Delta f)$ (see Fig. 1).

The proposed pilot-correlated PMD monitoring scheme has a number of advantages. First, as the frequency spacing between two adjacent optical subcarriers in the DDO-OFDM signal is quite small, the use of the proposed pilot correlation procedure can estimate the average power of one particular pilot subcarrier without the need of any narrowband filter, with good accuracy. Moreover, the DGD value is derived, via the power ratio of the two pilot subcarriers, instead of their absolute power values, thus the channel response, which may influence the power estimation, can be compensated. Furthermore, the proposed scheme only requires one photodiode, followed by simple electronic correlation operations, which make it a practical approach for PMD monitoring in a flexible optical network.

III. Experiment

Fig. 4 shows the experimental setup to verify our proposed PMD monitoring scheme. RF-tone-assisted gapped DDO-OFDM [14] was implemented. 256 subcarriers were used and 56 of them were modulated with data in 16-QAM formats. A strong RF tone was inserted at the leftmost subcarrier as the virtual optical carrier. Two pilot sequences were modulated at the first and the last data subcarriers, respectively. Cyclic prefix length was set to be 5% of the OFDM symbol period. Altogether, 1024 symbols were generated. Electrical pre-emphasis equalizers were used to compensate the roll-off fading of the digital-to-analog converter. The OFDM signal was then synthesized, via an arbitrary waveform generator (Tektronix AWG7122C), with a sampling rate of 12 GSample/s. Consequently, a 10-Gb/s data OFDM signal was generated. Taking the guard band for

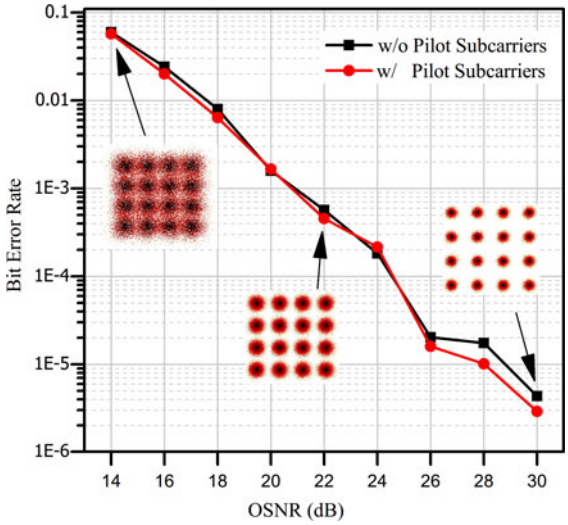

Fig. 5. BER performance for DDO-OFDM signal w/o and w/ pilot subcarriers insertion.

DDO-OFDM into account, the generated OFDM signal had a total bandwidth of about 5.5 GHz. The real and the imaginary parts of the output electrical OFDM signal were then converted to a single-sideband DDO-OFDM signal, via an optical IQ modulator, before being amplified by an erbium doped fiber amplifier (EDFA). A ProDelay^{TM} device was used as a DGD emulator, whose tunable range was from 0 to 45 ps. After fiber transmission, the received optical signal was first attenuated by variable optical attenuator (VOA), followed by an EDFA to adjust the OSNR. The optical signal was then detected, via a P-I-N photodiode with 10-GHz bandwidth. The detected electrical signal was sampled and stored by a real-time digital storage oscilloscope (DSO) (Tektronix DSA72004B). For each set DGD value, data were captured five times and averaged. Offline digital signal processing was employed to perform correlation between the designated pilot data sequences and the received signal. Then, the ratio of the estimated power, q, together with the frequency values of the two pilot sequence were used to calculate the DGD information using the proposed algorithm.

First, we investigated the impact of the insertion of two pilot subcarriers on the performance of the DDO-OFDM signal. Fig. 5 shows the respective measured bit error rate (BER) performance over different OSNR values in 100-km fiber transmission. The results showed that negligible impact due to the presence of the pilot subcarriers was observed. Then, we verified our proposed scheme in the presence of amplified spontaneous emission (ASE) noise. Fig. 6 shows the monitored DGD values versus the set DGD values, under four different OSNR (0.1-nm bandwidth) values of 15 dB, 20 dB, 25 dB and 30 dB, and showed good agreement. The received optical power at the photodiode was set to be -11 dBm in all measurements. As the additive ASE noise was uncorrelated with the pilot data sequence, their correlation results were much smaller than those between the pilot sequences and the signal, resulting in small fluctuations in the monitoring. The standard deviations of the monitoring error at each OSNR value were all below 2 ps.

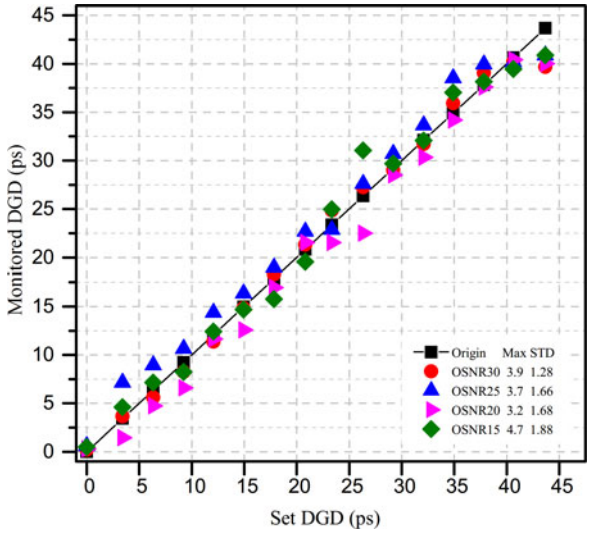

Fig. 6. Monitored DGD versus DGD value in the fiber link, under different OSNR values. "Max" stands for maximum monitoring error, while "STD" stands for standard deviation of monitoring error.

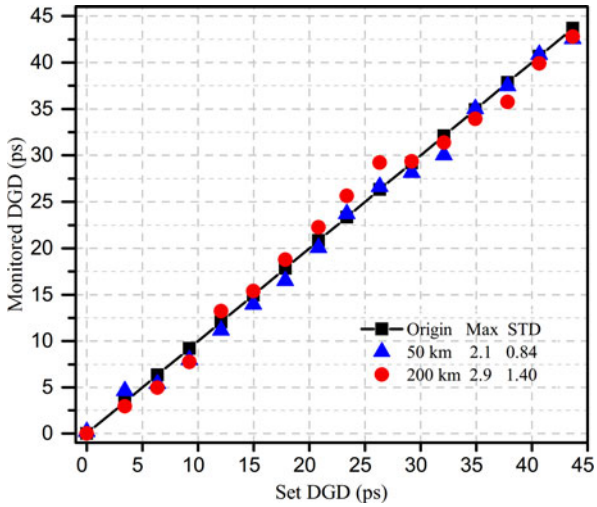

Fig. 7. Monitored DGD versus DGD value in the fiber link, with transmission length of 50 km and 100 km.

To investigate the robustness of this proposed PMD monitoring scheme against the accumulated chromatic dispersion (CD), fiber transmission of 50 km and 200 km were conducted. The OSNR was set to be 25 dB in these two cases and the received optical power at the photodiode was set to be −11 dBm.

Fig. 7 shows the DGD monitoring results and it was shown that CD induced power fading was negligible, which was attributed to the single-sideband of the DDO-OFDM signal. The standard deviations of monitoring errors were below 1.5 ps over the whole monitoring range.

IV. Discussion

A. Low Bandwidth Photodiode

Under normal optical signal detection, if the bandwidth of the photodiode is lower than the signal bandwidth, the out-of-band signal will suffer from large attenuation, which can be modeled as excessive filtering effect by a low pass filter. This filtering effect degrades frequency response to the converted electrical signal of photodiode. In order to employ a photodiode which has a much lower bandwidth than the signal bandwidth, it is required that the inserted pilot data sequence at higher frequency could still be detected by signal correlation after the severe signal attenuation due to much degraded frequency response of the photodiode. Besides, the correlation results have to be calibrated to obtain an accurate monitoring result.

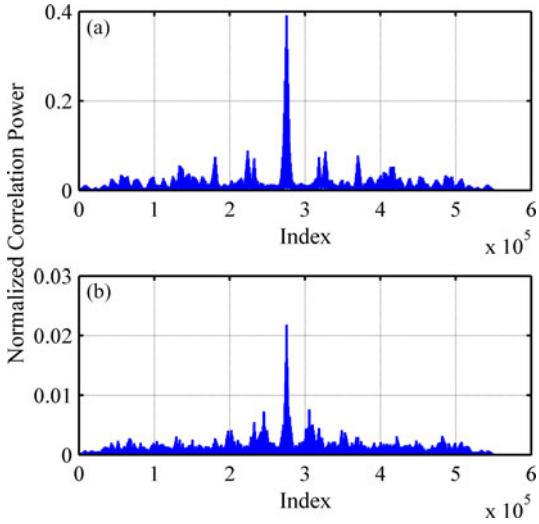

Fig. 8. Correlation peaks of (a) pilot subcarrier (PS) 1, (b) pilot subcarrier 2 with DGD = 0 ps. Photodiode of 1-GHz bandwidth is used.

In this investigation, the correlation result was measured using the same experimental setup, as shown in Fig. 4, except utilizing a photodiode with bandwidth of 1 GHz. The modulated OFDM signal has a bandwidth of about 5.5 GHz. Fig. 8 shows the correlation result of the pilot data sequences and the received data, when DGD was set to be 0 ps. It was shown that the correlation peaks were still salient, compared with the uncorrelated part. However, the correlation peak value of the second pilot sequence was severely attenuated, with a factor of about 24, as shown. It was mainly due to the high peak to average value of the correlation result.

With such excessive filtering at the high frequency region, the estimated values of a_1 and a_2, as in (3) and (4), will no longer be equal any more, even under zero DGD. Besides, the discrepancy is also dependent on the frequency response of the photodiode used, thus is device-specific. Therefore, the obtained correlation results have to be normalized by the reference power ratio of the two pilot subcarriers using the proposed pilot-correlation scheme, measured under zero DGD. Numerical simulation was first performed so as to prove the concept of the feasibility of using low-bandwidth photodiode in the proposed PMD monitoring scheme. A 3-order Bessel filter with its bandwidth varied from 1 GHz to 10 GHz was employed to simulate the low-bandwidth photodiode response, and it was used to filter the DDO-OFDM signal, having an effective bandwidth of 6 GHz (56 data subcarriers), before performing the

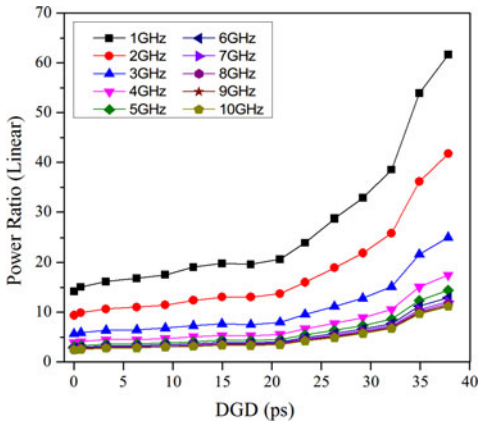

Fig. 9. Simulation results of power ratio of two pilot subcarriers w.r.t DGD values when the bandwidth of photodiode ranges from 1 GHz to 10 GHz (without calibration).

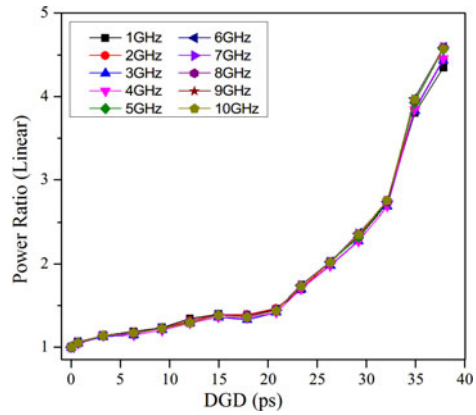

Fig. 10. Simulation results of power ratio of two pilot subcarriers w.r.t DGD values when the bandwidth of photodiode ranges from 1 GHz to 10 GHz. (With calibration).

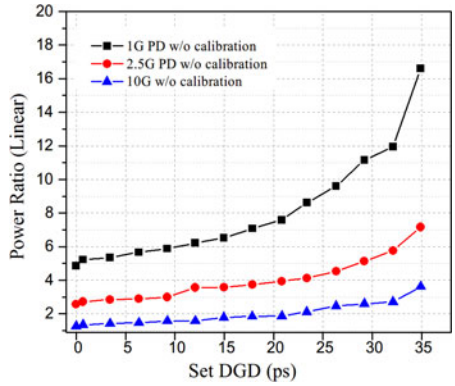

Fig. 11. Experimental results of power ratio of two pilot subcarriers w.r.t DGD values when the bandwidths of photodiode are 1 GHz, 2.5 GHz, and 10 GHz, respectively. (without calibration).

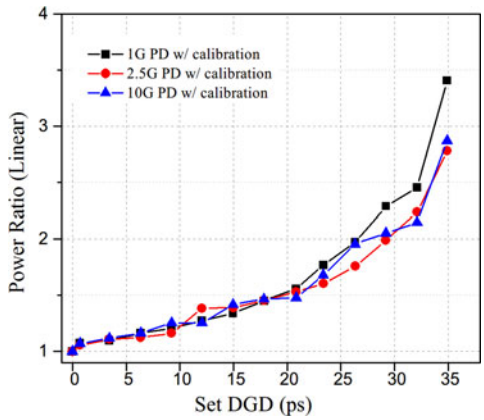

Fig. 12. Experimental results of power ratio of two pilot subcarriers w.r.t DGD values when the bandwidths of photodiode are 1 GHz, 2.5 GHz, and 10 GHz, respectively. (with calibration).

signal correlation procedures to estimate the signal's DGD value. Fig. 9 shows the simulation results, in which the absolute values of the power ratios of the two pilot subcarriers decreased when the bandwidth of the photodiode increased until it exceeded that of the DDO-OFDM signal. Fig. 10 plots the respective adjusted power ratios after the calibration was applied. Negligible fluctuation in the respective adjusted power ratios was observed when the DGD value was lower than 35 ps, which revealed the feasibility and effectiveness of the calibration method.

Fig. 11 shows the experimental measurements of the power ratios of the two pilot subcarriers in the received DDO-OFDM signal with photodiode bandwidths of 1 GHz, 2.5 GHz, and 10 GHz, respectively, without calibration. Meanwhile, Fig. 12 shows the calibrated power ratios. The OSNR was preserved to be 25 dB in all cases. The received powers before the photodiodes were set to be optimum. The results show that the curves of the cases having calibration were very close to each other, proving the effectiveness of the proposed calibration method. Fig. 13 shows the DGD monitoring results based on the calibrated DGD values, using photodiodes of 1-GHz, 2.5-GHz and 10-GHz bandwidths, and they all showed good agreement between the set DGD values and the monitored DGD values. The standard deviation of monitoring error was below 2 ps.

B. Input Angle of State of Polarization

All of the above investigations focus on the impact of the DGD induced by the fiber link on the optical signal. In such application, a polarization controller should be placed in front of a DGD element, to control the amplitude splitting ratio γ to be 0.5, such that the actual DGD effect on the optical signal equals the polarization mode dispersion of the DGD element. However, if the power of the slow and the fast axes are not identical, that is, the input angle between the input signal and the PSP of the DGD element is not 45°, the DGD effect on the optical signal is not identical to the exact value of the time difference between the two axes in the DGD element. In view of such phenomenon, a modified DGD monitoring scheme is proposed so that the monitoring results are independent of the value of the amplitude splitting ratio γ.

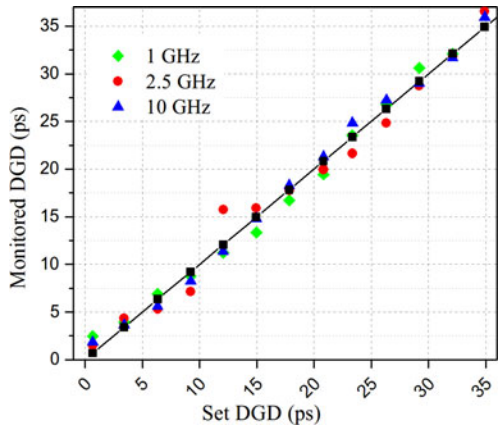

Fig. 13. Experimental results of monitored DGD values versus set DGD values when the bandwidths of photodiode are 1 GHz, 2.5 GHz, and 10 GHz, respectively. (With calibration).

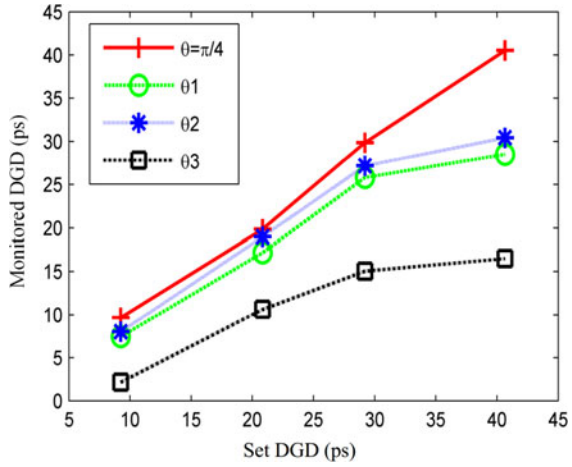

Fig. 14. Monitored DGD versus DGD of fiber link under different input angle for 2-pilot scheme.

By squaring both sides of (1), we can obtain,

$$|H(\omega_k, \gamma, \Delta\tau)|^2 = 2\gamma(1-\gamma)\cos(\omega_k \Delta\tau) + \gamma^2 + (1-\gamma)^2 \tag{11}$$

which contains a constant component, $\gamma^2 + (1-\gamma)^2$, and thus makes the simple power ratio between the two pilot subcarriers inapplicable to derive the DGD information accurately. One feasible solution is to employ three pilot subcarriers with distinct pre-known symbols. Suppose there are three frequency components f_1, f_2, f_3, with their corresponding magnitudes, A_1, A_2, A_3, then we have:

$$A_1^2 = 2\gamma(1-\gamma)\cos(\omega_1 \Delta\tau) + \gamma^2 + (1-\gamma)^2 \tag{12}$$

$$A_2^2 = 2\gamma(1-\gamma)\cos(\omega_2 \Delta\tau) + \gamma^2 + (1-\gamma)^2 \tag{13}$$

$$A_3^2 = 2\gamma(1-\gamma)\cos(\omega_3 \Delta\tau) + \gamma^2 + (1-\gamma)^2 \tag{14}$$

By combining (12), (13) and (14) together, we have,

$$\frac{A_1^2 - A_2^2}{A_2^2 - A_3^2} = \frac{\cos(\omega_1 \Delta\tau) - \cos(\omega_2 \Delta\tau)}{\cos(\omega_2 \Delta\tau) - \cos(\omega_3 \Delta\tau)} \tag{15}$$

Consequently, no γ remains in (15) and thus the DGD value can be calculated insensitive to γ, with the magnitudes A_1, A_2, A_3, being retrieved by the proposed pilot-correlation procedures, as discussed in Section II.

To verify the feasibility of this modified scheme using three pilot subcarriers, four different DGD values were tested experimentally, with three different arbitrary values of the input angle θ. Figs. 14 and 15 show the monitored DGD values versus set DGD values when two pilot-subcarriers and three pilot subcarriers were employed, respectively. The measured DGD values showed great variation in the former case (Fig. 14), while they showed little variance in the latter case (Fig. 15). We also conducted experiment verification by replacing the polarization controller with a polarization scrambler before DGD emulator, as in the experimental setup shown in Fig. 4. For each measurement, 10 random polarization was altered by the polarization scrambler, and the DGD was measured with our proposed 3-pilot scheme. The measurement result, with its monitoring errors was shown in Fig. 16. Less than 3-ps monitoring error was

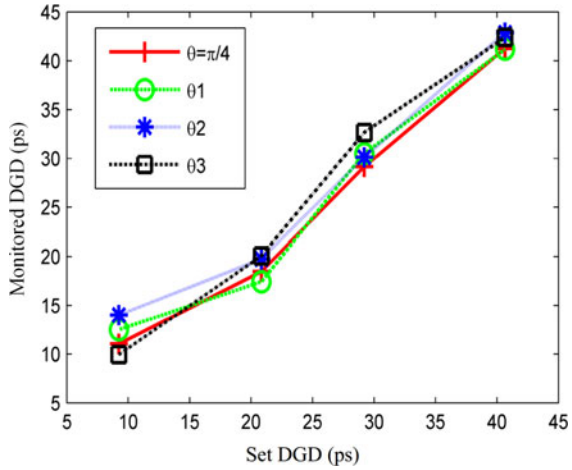

Fig. 15. Monitored DGD versus DGD of fiber link under different input angle for 3-pilot scheme.

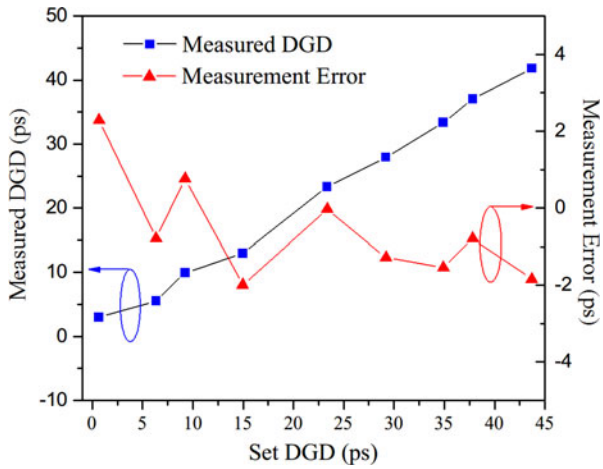

Fig. 16. Measured DGD and measurement error versus set DGD values.

observed. This confirmed the effectiveness of employing three pilot subcarriers in a DDO-OFDM signal to measure the DGD value of fiber under test insensitive to the input polarization.

C. Polarization Dependent Loss (PDL) Effect

PDL originates from the polarization sensitive devices in the system. PDL itself can cause frequency independent optical power fluctuations and random OSNR variations, due to polarization state wandering during propagation [15]. Besides, the mutual interaction of PMD and PDL may lead to additional system performance degradation since the two principal states of polarization are no longer orthogonal. Unlike the conventional RF power based PMD monitoring schemes, which were based on the absolute power of a particular RF tone, the fading introduced by pure PDL does not affect our first order PMD monitoring, as its effect is mitigated in (5) when calculating the power ratio. In general, it has been pointed out in [16] that for the current optical fibers and devices, which have relatively small values of DGD and PDL parameters, the interaction between PDL and PMD would become detrimental only in ultra-long-haul transmission system, which is not the case for most of the DDO-OFDM applications.

V. Summary

We have experimentally proposed and extensively characterized a first-order PMD monitoring scheme for DDO-OFDM system. By inserting two or three pilot subcarriers to the DDO-OFDM signal, the accumulated DGD value of received DDO-OFDM signal can be accurately monitored. The DGD monitoring range for a 10-Gbit/s RF-tone-assisted DDO-OFDM system was measured to be about 45 ps. The standard deviation of the monitoring error was below 2 ps. By using the proposed pilot-correlation method, simple DGD monitoring is realized without using narrowband optical/electrical filter. No coherent receiver is required. It has also been shown that a photodiode with bandwidth lower than the signal bandwidth can even be employed, at the expense of simple calibration. The low-complexity as well as high robustness against CD, OSNR and input angle to fiber, imply a strong potential of realizing practical PMD monitoring at the intermediate nodes in flexible optical networks.

References

[1] M. Jinno, H. Takara, B. Kozicki, Y. Tsukishima, Y. Sone, and S. Matsuoka, "Spectrum-efficient and scalable elastic optical path network: Architecture, benefits, and enabling technologies," *IEEE Commun. Mag.*, vol. 47, no. 11, pp. 66–73, Nov. 2009.

[2] W. Shieh, "OFDM for flexible high-speed optical networks," *J. Lightw. Technol.*, vol. 29, no. 10, pp. 1560–1577, May 2011.

[3] W. Shieh and C. Athaudage, "Coherent optical orthogonal frequency division multiplexing," *Electron. Lett.*, vol. 42, pp. 587–589, 2006.

[4] J. Armstrong and A. J. Lowery, "Power efficient optical OFDM," *Electron. Lett.*, vol. 42, no. 2, pp. 370–372, Mar. 2006.

[5] W. R. Peng, "Direct detection optical OFDM," presented at the Opt. Fiber Commun. Conf., San Francisco, CA, USA, 2014, Paper Th3K.7 (Invited).

[6] X. Xiao, T. Gui, S. You, Q. Yang, R. Hu, Z. He, M. Luo, C. Li, X. Zhang, D. Xue, Z. Li, X. Chen, and S. Yu, "432-Gb/s direct-detection optical OFDM superchannel transmission over 3040-km SSMF," *IEEE Photon. Technol. Lett.*, vol. 25, no. 15, pp. 1524–1526, Aug. 2013.

[7] J. Armstrong, "OFDM for optical communications," *J. Lightw. Technol.*, vol. 27, no. 3, pp. 189–204, Feb. 2009.

[8] B. C. Schmidt, A. Lowery, and J. Armstrong, "Experimental demonstrations of electronic dispersion compensation for long-haul transmission using direct-detection optical OFDM," *J. Lightw. Technol.*, vol. 26, no. 1, pp. 196–203, Jan. 2008.

[9] M. Mayrock and H. Haunstein, "PMD tolerant direct-detection optical OFDM system," presented at the Eur. Conf. Opt. Commun., Berlin, Germany, 2007.

[10] X. Yi, W. Shieh, Y. Ma, Y. Tang and G. J. Pendock, "Experimental demonstration of optical performance monitoring in coherent optical OFDM systems," presented at the Opt. Fiber Commun. Conf./Nat. Fiber Opt. Eng. Conf., San Diego, CA, USA, 2008, Paper OThW3.

[11] C. C. Do, A. V. Tran, S. Chen, T. Anderson, D. Hewitt, and E. Skafidas, "Flexible bandwidth DGD estimation for coherent optical OFDM system," *Opt. Exp.*, vol. 21, pp. 25788–25795, Nov. 2013.

[12] T. Bo, S. Gao, K. Tse, and C. Chan, "A PMD monitoring scheme for direct-detection optical OFDM systems using code-assisted optical subcarriers," presented at the Conf. Lasers Elect.-Opt., San Jose, CA, USA, 2014, Paper STu3J.4.

[13] N. Cvijetic, S. G. Wilson, and D. Qian, "System outage probability due to PMD in high-speed optical OFDM transmission," *J. Lightw. Technol.*, vol. 26, no. 14, pp. 2118–2127, Jul. 2008.

[14] W. Peng, X. Wu, V. R. Arbab, K. Feng, B. Shamee, L. C. Christen, J. Yang, A. Willner, and S. Chi, "Theoretical and experimental investigations of direct-detected RF-tone-assisted optical OFDM systems," *J. Lightw. Technol.*, vol. 27, no. 10, pp. 1332–1339, Apr. 2009.

[15] A. E. Willner, S. M. R. M. Nezam, L. Yan, Zhongqi Pan, and M. C. Hauer, "Monitoring and control of polarization-related impairments in optical fiber systems," *J. Lightw. Technol.*, vol. 22, no. 1, pp. 106–125, Jan. 2004.

[16] R. Feced, S. J. Savory, A. Hadjifotiou, J. Jiang, D. Richards, S. Oliva, P. Green, and R. Hui, "Interaction between polarization mode dispersion and polarization-dependent losses in optical communication links; PMD and PDL monitoring of traffic-carrying transatlantic fibre-optic system," *J. Opt. Soc. Amer. B*, vol. 20, no. 45, p. 424, 2003.

Authors' biographies not available at the time of publication.